Variable-Temperature Electrical Measurements of Zinc Oxide/Tin Oxide-Cosubstituted Indium Oxide

A. Ambrosini, G. B. Palmer,† A. Maignan,‡ and K. R. Poeppelmeier*

Department of Chemistry, Northwestern University, Evanston, Illinois 60208-3113

M. A. Lane, P. Brazis, and C. R. Kannewurf

Department of Electrical and Computer Engineering, Northwestern University, Evanston, Illinois 60208-3118

T. Hogan

Electrical and Computer Engineering and Materials Science and Mechanics, Michigan State University, East Lansing, Michigan 48824

T. O. Mason

Department of Materials Science and Engineering, Northwestern University, Evanston, Illinois 60208-3105

Received January 29, 2001. Revised Manuscript Received October 2, 2001

The electrical conductivity, Hall effect, and thermoelectric coefficient of Zn/Sn-cosubstituted In_2O_3 ($In_{2-2x}Sn_xZn_xO_{3-\delta}$), undoped In_2O_3, and indium−tin oxide (ITO) were studied vs cation composition, state of reduction, and measurement temperature (over the range of 4.2−340 K). Carrier contents and mobilities were determined from the Hall coefficient and conductivity in each case. $In_{2-2x}Sn_xZn_xO_{3-\delta}$ displays conductivities up to 1 order of magnitude lower than ITO, and the conductivity of the material decreases with increasing cosubstitution, from approximately 860 to 235 S/cm. Reduction of the materials under flowing H_2/N_2 increases their carrier concentrations and therefore their conductivities. These results are discussed in terms of possible defect and transport models.

Introduction

Transparent conducting oxides (TCOs) are materials that combine visual light transparency and high electrical conductivity. Device manufacturers use TCO films as transparent electrodes in solar cells, flat panel displays, and many other applications. The commercial TCO of choice, tin-doped indium oxide (ITO) has a typical conductivity of $1-5 \times 10^3$ S/cm and a transparency of 85−90% in thin films.[1,2] Although ITO meets the needs of current devices, researchers continue to look for improved TCO films based on new chemical compositions. Recently, several new TCOs with properties similar to ITO have been reported.[3−5]

Although most TCO applications require thin films, bulk investigations complement thin film research. Specifically, bulk synthesis allows careful control of complex stoichiometries, which is useful in the investigation of fundamental structure−property relationships. In addition, bulk investigations are directly relevant to the sintering of targets for thin film deposition and certain applications, such as paper additives. Caution should be taken in comparing film and bulk results because of potential differences in phase chemistry and microstructure.

While constructing the $In_2O_3-SnO_2-ZnO$ subsolidus phase diagram,[6] a large new In_2O_3-based solid solution range was discovered.[7] Cosubstitution of In_2O_3 by ZnO and SnO_2 raised the solubility of each from approximately 0 and 6%, respectively, to approximately 20% for each (40% total). The cosubstituted material displays electrical conductivity that is 2−3 orders of magnitude higher than that of undoped In_2O_3 but 1 order of magnitude lower than that of ITO. UV−visible (UV−vis) diffuse reflectance measurements show that cosubstitution causes a reduction of the band gap.

* To whom correspondence should be addressed. E-mail: krp@northwestern.edu.

† Present address: McKinsey & Company, Inc., 133 Peachtree St., STE 4600, Atlanta, GA 30303.

‡ Permanent address: Laboratoire CRISMAT-ISMRA-U. M. R. C.N.R.S. 6508-Boulevard du Maréchal Juin-14050 CAEN cédex France.

(1) Hamberg, I.; Granqvist, C. G. *J. Appl. Phys.* **1986**, *60*, R123.

(2) Lynam, N. R. In *Symposium on Electrochromic Materials*; Carpenter, M. K., Corrigan, D. A., Eds.; Electrochemical Society, 1990; Vol. 90, pp 201−231.

(3) Palmer, G. B.; Poeppelmeier, K. R.; Edwards, D. D.; Mason, T. O. *Proc. Mater. Res. Soc. Spring 1998, Symp. B: Flat Panel Display Mater. Large Area Processes* **1998**, *508*, 308.

(4) Minami, T.; Takata, S.; Kakumu, T. *J. Vac. Sci. Technol., A* **1996**, *14*, 1689.

(5) Wang, R. P.; Sleight, A. W.; Platzer, R.; Gardner, J. A. *J. Mater. Res.* **1996**, *11*, 1659.

(6) Phillips, J. M.; Cava, R. J.; Thomas, G. A.; Carter, S. A.; Kwo, J.; Siegrist, T.; Krajewski, J. J.; Marshall, J. H.; Peck, W. F.; Rapkine, D. H. *Appl. Phys. Lett.* **1995**, *67*, 2246.

(7) Palmer, G. B.; Poeppelmeier, K. R.; Mason, T. O. *Chem. Mater.* **1997**, *9*, 3121.

10.1021/cm0100725 CCC: $22.00
Published on Web 12/13/2001

Relative transparency at 500 nm is similar to or slightly greater than that of ITO.

In this work, the relationships between transport properties (i.e., carrier concentration and mobility) and chemical state (i.e., cation composition and state of reduction) were investigated in Zn/Sn-cosubstituted In_2O_3 ($In_{2-2x}Sn_xZn_xO_{3-\delta}$). For comparison purposes, identical measurements were made on undoped and Sn-doped In_2O_3 (ITO). In addition, several defect and transport models were considered.

Experimental Section

Synthesis, Density, and X-ray Crystallography. Sample pellets were synthesized by using conventional solid-state reaction techniques as described previously,[7] with three exceptions. (1) Samples were fired for a shorter time at 1250 °C (1 day for ZnO-containing samples) to minimize ZnO evaporation. (2) Samples were "air-quenched" by removing the sample crucible from the furnace into the ambient laboratory air. (3) Selected pellets were reduced in flowing forming gas (7% H_2/93% N_2) for 10 h at 500 °C.

Sample densities were calculated from the ratio of pellet mass and volume. Pellet volumes were estimated by measuring diameter and thickness of the cylindrical pellets by caliper. Measured pellet densities were approximately 50% of the theoretical crystal density, and the variation of density among samples was within measurement uncertainty. In this study, higher temperatures or sintering times were not used to increase densification because of concerns about ZnO volatility.

Powder X-ray diffraction patterns were collected by using copper Kα radiation at 40 kV and 20 mA (Rigaku, USA) from $2\theta = 10-70°$.

Room-Temperature Electrical Measurements. Room-temperature electrical conductivities of as-fired pellets were measured with a spring-loaded linear four-probe apparatus described previously.[7,8] The correction factors of Smits were used to adjust for the geometry of the disc-shaped, pelletized samples.[9] No corrections were made for porosity; uncorrected conductivities will be discussed throughout.

Low-Temperature Electrical Measurements. Electrical conductivity and dc Hall measurements were taken from 4.2 to 340 K by using a computer-controlled five-probe technique.[10] Samples were cooled to 4.2 K, and measurements were taken as the system warmed to 290 K. From 290 to 340 K, a heater was used to raise the temperature. The voltage-sensing electrodes were 25 μm gold wire, placed approximately 0.5 cm apart. The sensing contacts on the samples were prepared with indium dots. The gold electrode wires were attached to the contacts with silver paste. On these materials, voltage contacts made with indium and silver paste were found to be superior to those made with only gold or silver paste. The current electrodes were 60 μm gold wire and were attached to the ends of the samples with gold paste. Hall measurements were performed with 7400 G magnetic flux density and 100 mA applied current. All voltages were measured with a Keithley 181 nanovoltmeter. The relationship $1/ne = R_H$ (where n is carrier concentration, e is the electron charge, and R_H is the Hall coefficient) was used to determine carrier concentrations.

Variable-temperature thermopower measurements were taken by using a computer-controlled slow ac technique from 4.2 to 295 K.[11,12] During the measurements, the samples were kept in a 10^{-5} Torr vacuum. The samples were attached with gold paste to two 60 μm gold wires, which were attached to separate quartz blocks with heaters. Temperature gradients of 0.1−0.4 K were applied and measured with Au (0.07% Fe)/chromel differential thermocouples. The voltage electrodes, 10 μm gold wires, were made as long as possible to minimize heat conduction through the leads. The sample and thermocouple voltages were measured with Keithley 181 and Keithley 182 nanovoltmeters, respectively.

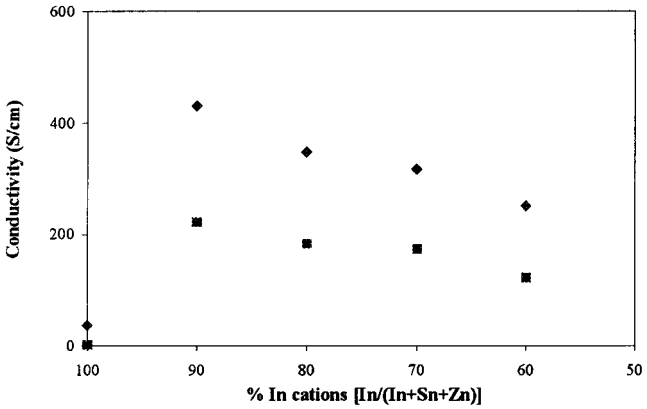

Figure 1. ZnO/SnO_2-cosubstituted In_2O_3. Conductivity vs cation % In of as-fired (▲) and reduced (■) samples.

For conductivity and Hall measurements, rectangular bar-shaped samples (approximately 1.25 × 1 × 10 mm) were prepared by cutting the as-fired pellets with a diamond saw. The ITO bar-shaped sample was obtained by pressing and firing a rectangular sample.

dc Susceptibility. The dc susceptibility of the ceramic samples was obtained from magnetic measurements performed with a Quantum Design SQUID susceptometer. The sample was first zero-field-cooled to 5 K after which a magnetic field of 50 G was applied. Measurements were taken as the temperature was cycled between 5 K and $T > T_C$, where T_C is the critical temperature of susceptibility, while maintaining the magnetic field. Isothermal magnetization vs field measurements on samples which were first zero-field-cooled were collected at 2 K while cycling the field between 0 and 50 000 G.

Results and Discussion

X-ray Phase Analysis. In_2O_3 (JCPDS Card No. 6-416) crystallizes in the *C*-type rare earth (bixbyite) structure.[13] The unit cell is body-centered cubic (space group *Ia*-3) with lattice parameter $a = 10.117(1)$ Å. When SnO_2 substitutes in In_2O_3 (ITO) or ZnO and SnO_2 cosubstitute in $In_{2-2x}Sn_xZn_xO_{3-\delta}$, the crystal structure remains cubic and the lattice parameter expands (ITO) or contracts (cosubstitution). Cosubstitution gives a Vegard's law (linear) trend of lattice parameter vs composition.[7] All samples in this study were single-phase bixbyite as assessed by X-ray powder diffraction.

Room-Temperature Conductivity. The electrical conductivity vs amount of Zn/Sn cosubstitution is shown in Figure 1. Except for the initial rise from undoped $In_2O_{3-\delta}$ to the 10% cosubstituted specimen, conductivity decreased with increasing cosubstitution, as previously reported.[7] In separate work, in situ conductivity measurements were used to examine the effects of time and temperature during reduction of $In_2O_{3-\delta}$, ITO, and cosubstituted $In_2O_{3-\delta}$ by forming gas. That study showed that the reduction scheme used here (10 h at 500 °C) resulted in the highest conductivities and did not cause the over-reduction of the oxides to metals. To ensure

(8) Moriga, T.; Edwards, D. D.; Mason, T. O.; Palmer, G. B.; Poeppelmeier, K. R.; Schindler, J. L.; Kannewurf, C. R.; Nakabayashi, I. *J. Am. Ceram. Soc.* **1998**, *81*, 1310.
(9) Smits, F. M. *Bell Syst. Tech. J.* **1958**, *37*, 711.
(10) Lyding, J. W.; Marcy, H. O.; Marks, T. J.; Kannewurf, C. R. *IEEE Trans. Instrum. Meas.* **1988**, *37*, 76.
(11) Chaikin, P. M.; Kwak, J. F. **1975**, *46*, 218.
(12) Marcy, H. O.; Marks, T. J.; Kannewurf, C. R. *IEEE Trans. Instrum. Meas.* **1990**, *39*, 756.
(13) Marezio, M. *Acta Crystallogr.* **1966**, *20*, 723.

Table 1. Carrier Concentrations and Mobilities[a]

description	carrier concn ($\times 10^{20}$ cm^{-3})	mobility (cm^2/V·s)
as-fired ITO	3.3(0.7)	38(6)
reduced cosubstituted (90% In)	7.0(0.8)	14(1)
reduced cosubstituted (70% In)	3.2(0.9)	13(3)
reduced cosubstituted (60% In)	3.4(2.7)	14(8)
as-fired cosubstituted (95% In)	3.0(0.4)	18(2)
as-fired cosubstituted (85% In)	2.3(0.4)	22(3)
as-fired cosubstituted (80% In)	2.0(0.4)	29(6)
as-fired cosubstituted (75% In)	2.3(0.5)	18(4)
as-fired cosubstituted (60% In)	1.7(0.2)	21(2)

[a] Calculated from averaging data over the range of 4−290 K. Standard deviations in parentheses.

that the cosubstituted pellets underwent the same reduction conditions, they were reduced simultaneously. Figure 1 shows the effect of this reduction process on the conductivities of cosubstituted $In_{2-2x}Sn_xZn_xO_{3-\delta}$ ($0 < x < 0.4$). Reduction raised the conductivity of each sample by 80−110% but preserved the general conductivity vs cosubstitution trend. For comparison, the conductivity of undoped $In_2O_{3-\delta}$ was about 2 orders of magnitude less than that of 10% cosubstituted In_2O_3, while that of ITO (4% Sn) was significantly higher (936 S/cm as-fired, 1768 S/cm reduced).

It must be stressed that the conductivities in this work were not corrected for the nearly 50% porosity in the specimens. Employing standard mixing law models for 3−3 microstructures (i.e., matrix and pores both interconnected in 3-D)[14] we anticipate true conductivities to be a factor of 3−4 times larger. Nevertheless, the raw conductivities can still be used to evaluate relative doping and reduction effects in these materials.

Point Defect Mechanisms. Indium oxide is a wide band gap (~3.5 eV) semiconductor. If perfectly stoichiometric, the material should have insignificant carrier content at room temperature. While sample impurities (inadvertent dopants) are a potential source of carriers in the "pure" material, carrier concentrations on the order of 10^{18} cm^{-3} (approximately 2 orders of magnitude less than those in Table 1) are too high to be explained by inadvertent doping by cation impurities. It has been proposed that indium oxide is oxygen deficient; i.e., the oxygen nonstoichiometry can be expressed by delta (δ) in the formula $In_2O_{3-\delta}$.[15] This is supported by the increased conductivity of the reduced $In_2O_{3-\delta}$ in the present work. Assuming that each vacancy donates two electrons to the carrier concentration, it would be expected that the oxygen vacancies generate carriers in the relation: $n = 2\delta$.

In this paper, "doped" In_2O_3 implies that the material has been intentionally doped with an aliovalent cation. The "undoped" material may contain oxygen vacancies and hence is written as "$In_2O_{3-\delta}$". In ITO, aliovalent tin doping and oxygen off-stoichiometry can coexist. In this case, however, Frank and Kostlin have shown the oxygen off-stoichiometry in ITO to be negative ($\delta < 0$) rather than positive ($\delta > 0$) as in undoped (i.e., no cation doping) $In_2O_{3-\delta}$.[16] In comparison to the parent fluorite structure, the bixbyite structure has ordered (structural)

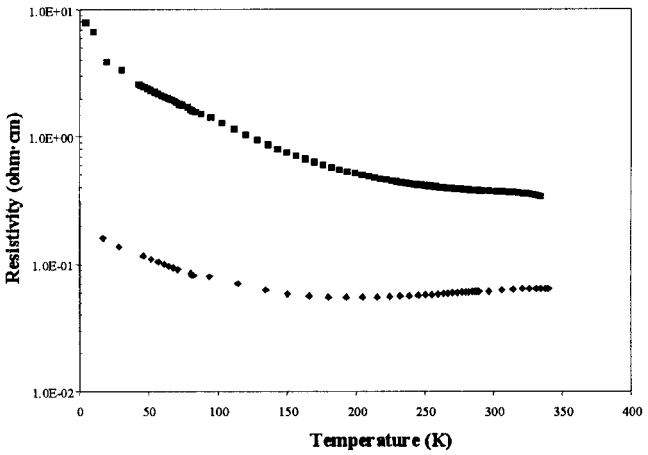

Figure 2. Resistivity vs temperature for as-fired (■) and reduced (♦) In_2O_3.

oxygen vacancies[13] which can readily accommodate interstitial oxygen ions. Tin donors and oxygen interstitial acceptors tend to be self-compensating through the formation of neutral point defect associates. Therefore, the oxygen interstitials are not reflected in the electroneutrality condition. Upon reduction, however, oxygen can be removed from some of these complexes, freeing the tin defects to act as donors, thereby increasing the electron population. This model of Frank and Kostlin has been supported recently by high-temperature transport measurements[17] and Rietveld analysis of neutron diffraction data on quenched specimens, confirming the existence of oxygen interstitials in oxidized ITO.[18]

In cosubstituted In_2O_3 ($In_{2-x-y}Sn_xZn_yO_{3-\delta}$), carriers may similarly come from two sources: excess Sn ($x > y$) or oxygen deficiency ($\delta > 0$). The total amount of expected carriers per formula unit is $(x - y) + 2\delta$, keeping in mind that δ must be positive (oxygen vacancies) to generate carriers; negative values of δ associated with oxygen interstitials are not reflected in the electroneutrality condition due to the neutrality of the defect complexes involved. Furthermore, only the quantity of excess Sn *not* tied up in associates, $(x - y)_{eff}$, is effective in donating electrons. Reduction of oxygen-excess materials removes the oxygen interstitials from defect associates, thereby increasing the value of $(x - y)_{eff}$. In our cosubstituted samples, x and y are nominally equal. However, slight Sn excesses may result from ZnO evaporation during heating or may be inherent to the exact phase boundary of the solid solution. The increase in conductivity of the reduced cosubstituted materials in Figure 1 is probably associated with removal of oxygen interstitials from excess tin complexes (given the large, ITO-like values of carrier content in Table 1); however, the production of oxygen vacancy donors cannot be ruled out. Rietveld analysis of neutron diffraction data should be able to detect whether oxygen interstitials are present and how their population changes with reduction.

Variable-Temperature Electrical Measurements. Figure 2 shows the temperature dependence of resistiv-

(14) McLachlan, D. S.; Blaszkiewics, M.; Newnham, R. E. *J. Am. Ceram. Soc.* **1990**, *73*, 2187.
(15) DeWit, J. H. W. *J. Solid State Chem.* **1973**, *8*, 142.
(16) Frank, G.; Kostlin, H. *Appl. Phys. A: Mater. Sci. Process.* **1982**, *27*, 197.
(17) Hwang, J. H.; Edwards, D. D.; Kammler, D. R.; Mason, T. O. *Solid State Ionics* **2000**, *129*, 135.
(18) Gonzalez, G. B.; Cohen, J. B.; Hwang, J. H.; Mason, T. O.; Hodges, J. P.; Jorgensen, J. D. *J. Appl. Phys.* **2001**, *89*, 2550.

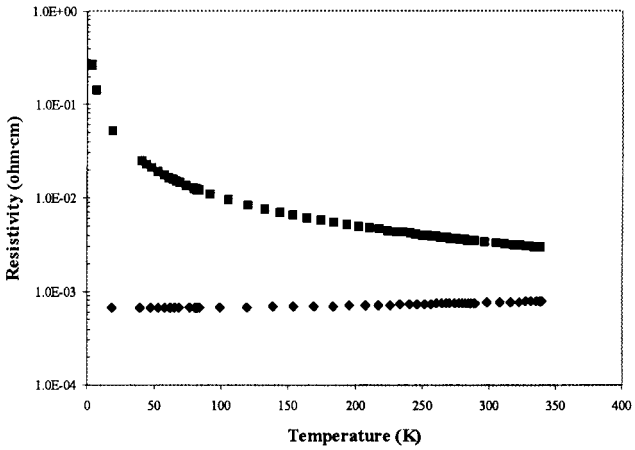

Figure 3. Low-temperature resistivity of as-fired (■) and reduced (♦) ITO.

ity for reduced and as-fired $In_2O_{3-\delta}$. While the resistivity of as-fired $In_2O_{3-\delta}$ decreased gradually with increasing temperature (semiconducting behavior), the reduced material showed a transitional character. Above 200 K, its resistivity increased with increasing temperature (metallic behavior); below 200 K, the opposite trend was observed. In terms of conductivity, reduction yielded a marked increase from 2.7 S/cm at 290 K for the as-fired sample to 16.3 S/cm for the reduced material, most likely due to the formation of oxygen vacancies as described above.

Figure 3 shows the temperature-dependent resistivity of as-fired and reduced ITO (4 cationic % Sn). The as-fired material displayed a pronounced decrease in resistivity with increasing temperature (semiconducting behavior). In contrast, the resistivity of the reduced ITO was virtually temperature independent from 4 to 100 K and gradually increased in an approximately linear fashion from 100 to 290 K (metallic behavior). Both the shape of the resistivity vs temperature curve and the overall magnitude of resistivity ($\sim 2.5 \times 10^{-4}$ Ω cm) are similar to previous measurements on ITO thin films.[19]

Figure 4 shows the temperature-dependent resistivity of as-fired, cosubstituted $In_{2-2x}Sn_xZn_xO_{3-\delta}$ of varying x. Above 200 K, the samples exhibited nearly linear increases in resistivity with increasing temperature. However, there is no observable trend in slope vs composition. Below 150 K, the resistivities either become essentially constant (the 5 and 15% cosubstituted samples) or increase slightly with decreasing temperature (the 25 and 40% cosubstituted samples), i.e., weak semiconductor-like behavior.

In Figure 5, the temperature-dependent resistivities of reduced, cosubstituted $In_{2-2x}Sn_xZn_xO_{3-\delta}$ ($x = 0.1$, 0.3, 0.4) are plotted. As with the reduced ITO in Figure 3, each sample exhibited essentially temperature-independent behavior below 100 K and a gradual linear increase in resistivity with increasing temperature from 100 to 290 K. The slope of the 100−290 K data increased with increasing level of cosubstitution.

The resistivity vs temperature graph for as-fired and reduced $In_{1.2}Sn_{0.4}Zn_{0.4}O_{3-\delta}$ is shown in Figure 6. The negligible slopes of the curves show that the resistivity

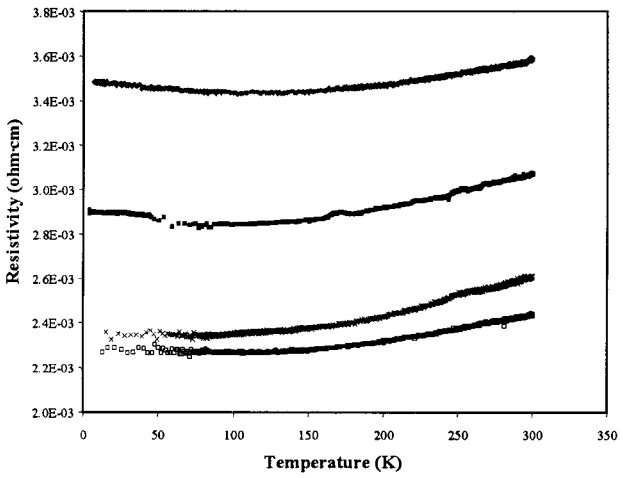

Figure 4. Low-temperature resistivity of as-fired, ZnO/SnO_2-cosubstituted $In_2O_{3-\delta}$ of various compositions: 95% In (□), 85% In (×), 75% In (■), and 60% In (♦).

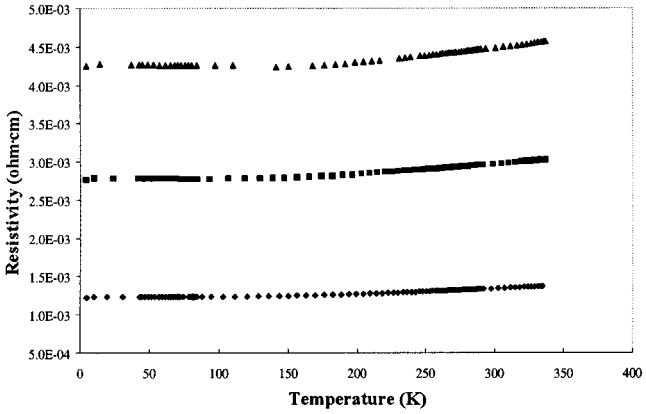

Figure 5. Low-temperature resistivity of reduced, ZnO/SnO_2-cosubstituted In_2O_3 of various compositions: 90% In (♦), 70% In (■), and 60% In (▲).

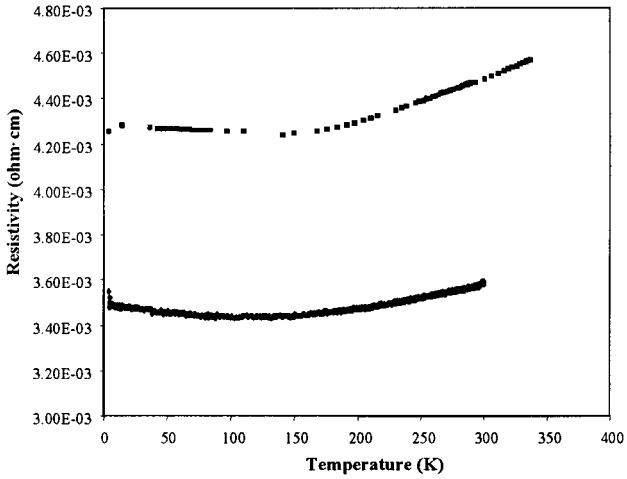

Figure 6. Low-temperature resistivity of same composition as-fired (♦) and reduced (■) (60% In) ZnO/SnO_2-cosubstituted In_2O_3.

is almost temperature independent. There is a slight change in slope from metal- to insulator-like behavior as the temperature decreases. This transition, which occurs at approximately 170 K, can be observed in strongly degenerate semiconductors.[20] Several transport models, including small polaron (adiabatic and nonadiabatic) and variable-range hopping, were tested on as-

(19) Zhang, D. H.; Ma, H. L. *Appl. Phys. A*: *Mater. Sci. Process.* **1996**, *62*, 487.

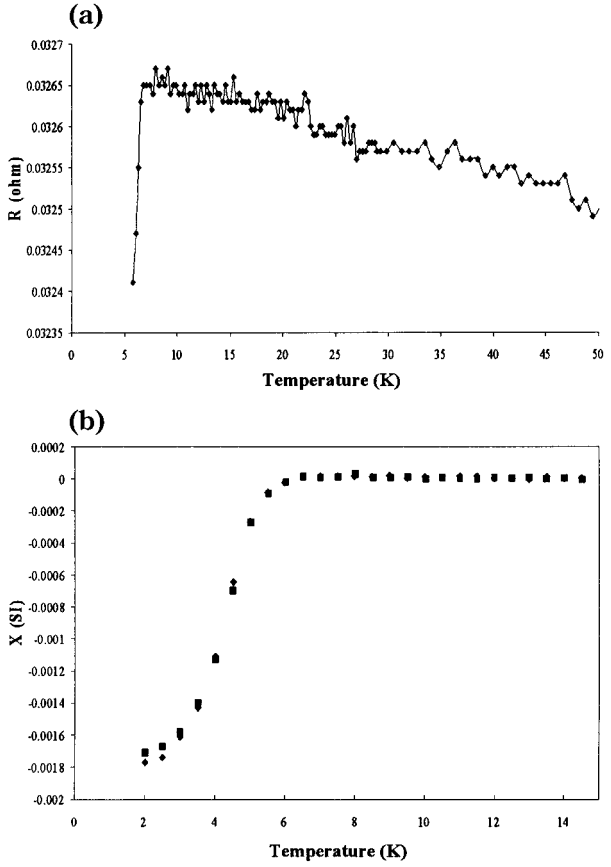

Figure 7. $In_{2-2x}Sn_xZn_xO_{3-\delta}$ ($x = 0.2$) low-temperature resistivity (a) and magnetic susceptibility (b) for field-cooled (■) and zero-field-cooled (♦) samples.

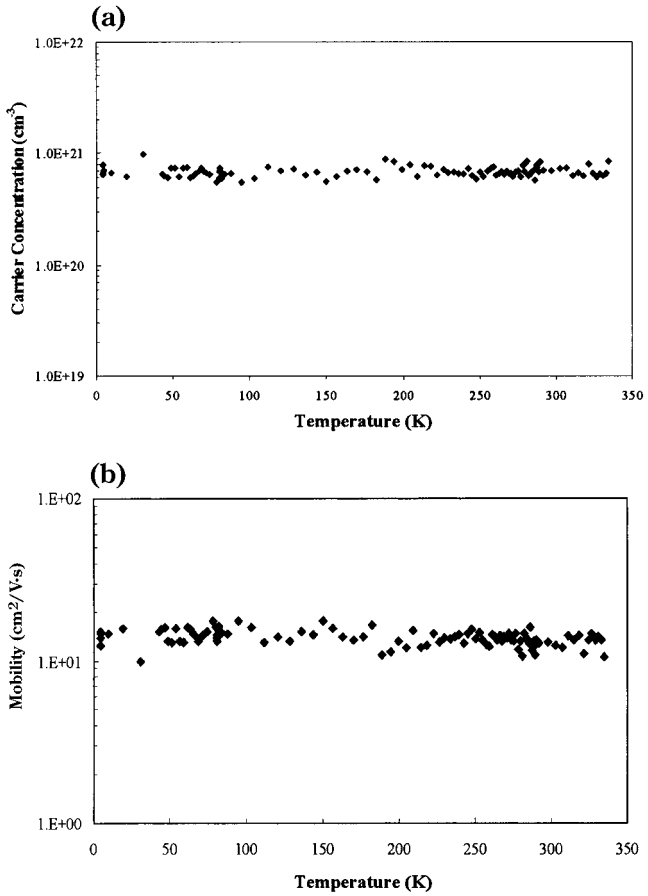

Figure 8. Carrier concentration (a) and mobility (b) vs temperature for reduced $In_2O_{3-\delta}$.

fired $In_{1.2}Sn_{0.4}Zn_{0.4}O_{3-\delta}$, which displayed the most prominent semiconductor-like region; however, none of the models was successful in fitting the observed behavior.

Magnetic Measurements. Low-temperature electrical and magnetic measurements indicated that the resistance of the reduced cosubstituted materials decreased substantially below about 6.5 K (Figure 7a), accompanied by a diamagnetic transition at the same temperature (Figure 7b). These results imply the possible onset of superconductivity for a small fraction of the material (0.04−0.7%). The resistivity transition is not complete at 4.2 K as shown in the resisitivity drop of only 0.8% in Figure 7a, which is related to the low diamagnetic volume fraction at the same temperature. The possible superconductivity may originate from a metallic impurity in the samples, as all three metals (In, Sn, and Zn) are superconductors at low temperatures, although their T_C's are lower than those observed here. Lead, which has a T_C near 6.5 K, was considered as a possible impurity in tin, on the basis of their chemical similarity. However, ICP analyses showed insignificant Pb in any of the starting material oxides. In addition, from the isothermal magnetization measurements collected at 2 K, a type II superconductivity is observed, which does not support the hypothesis of an elemental superconductor. However, an In−Sn alloy (formed from over-reduction) has not yet been ruled out as a source of the superconductivity.

(20) Mott, N. F. *Metal-Insulator Transitions*; Taylor and Francis: London, 1990.

Hall Effect of ITO, $In_2O_{3-\delta}$, and $In_{2-2x}Sn_xZn_xO_{3-\delta}$. Variable-temperature Hall effect measurements were taken to determine the respective roles of mobility and carrier concentration on the electrical conductivity. Hall effect measurements are difficult on highly conductive ceramic bulk samples because the Hall voltage is inversely proportional to the carrier concentration and the sample thickness. Hall voltages from highly conductive samples in this study were on the order of 100 nV. Although the nanovoltmeter was capable of measuring these voltages accurately, other sources of noise in the contacts and cabling interfered with precise measurements at low voltages.

Figure 8 shows the carrier concentration (a) and mobility (b) for reduced $In_2O_{3-\delta}$. In $In_2O_{3-\delta}$ as well as in cosubstituted $In_{2-2x}Sn_xZn_xO_{3-\delta}$, carrier concentration was typically flat over the entire temperature range. Variations in carrier concentration were usually 10−20% of the absolute value, dominated mainly by background noise. Consequently, the variable-temperature mobility data are also noisy, which may have obscured subtle trends vs temperature. In contrast, the resistivity measurements showed good signal-to-noise levels (usually under 1%) and revealed subtle trends vs temperature.

Assuming a temperature-independent carrier concentration, the region of linear resistivity vs temperature above 200 K for many of the samples in the present work (Figures 4 and 5) can be understood as being due to decreased mobility, arising from increased scattering at higher temperatures. Low-noise Hall effect measure-

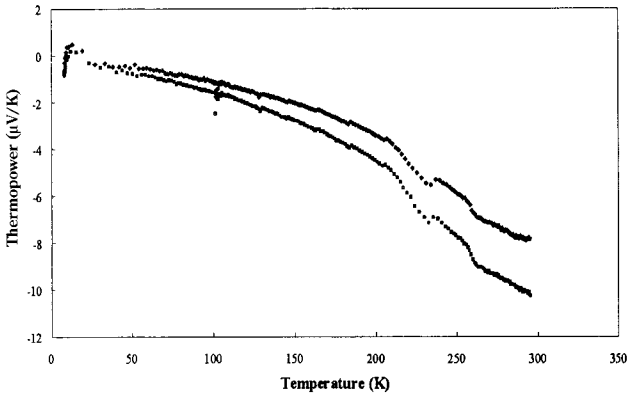

Figure 9. Low-temperature thermopower of as-fired $In_{1.9}Sn_{0.05}Zn_{0.05}O_{3-\delta}$.

ments on ITO films showed a similar correlation of mobility and conductivity in this region.[19]

Table 1 shows the carrier concentrations and mobilities of the variously treated specimens in the current work. The values were calculated by averaging the data sets over the entire temperature range of measurement. On an absolute scale, there were minimal changes in carrier concentration and mobility from 4.2 to 330 K. These differences were far less than the differences between samples. The sign of the Hall coefficient indicated that all samples were n-type.

In comparison to ITO, all of the cosubstituted samples had lower mobilities. This is reasonable based on the large number of ionized scattering centers introduced as a result of the cosubstitution. The unreduced cosubstituted samples had carrier concentrations between 1.7×10^{20} and 3.0×10^{20} cm^{-3} and mobilities of 18−31 $cm^2/V\cdot s$. The reduced cosubstituted samples displayed higher carrier concentrations of $(3.2-7.0) \times 10^{20}$ cm^{-3} and lower mobilities of 13−14 $cm^2/V\cdot s$. In general, carrier concentration increased as cosubstitution decreased. The reason for this is unclear at the present time.

Thermopower of Unreduced Cosubstituted In_2O_3. Figure 9 shows the thermopower of two samples of identical composition, $In_{1.9}Sn_{0.05}Zn_{0.05}O_{3-\delta}$. The sign of the thermopower also indicated n-type conduction. The samples appeared to be metallic throughout the temperature range. However, the thermopower vs temperature relationship showed a negative curvature (nonconstant slope). This appeared to correlate roughly with the corresponding change in resistivity vs temperature slope in Figure 5.

Conclusions

Although the cosubstitutions studied in this work are nominally isovalent with the host (Zn^{2+}/Sn^{4+} for $2In^{3+}$), as-fired materials showed levels of conductivity closer to that of ITO (within half an order of magnitude) than to that of undoped $In_2O_{3-\delta}$, which is smaller by 2 orders of magnitude. This suggests that excess Sn (i.e., $x > y$ in $In_{2-x-y}Sn_xZn_yO_{3-\delta}$), whether due to Zn evaporation during firing or inherent cation nonstoichiometry associated with the bixbyite phase field in the $In_2O_3-SnO_2-ZnO$ phase diagram, plays a major role in determining electron population. Furthermore, the ability to enhance carrier content by reduction suggests that a number of the Sn donors are tied up in neutral defect complexes with oxygen interstitials, as originally reported for ITO. Reduction may dissociate some of these defects by the removal of excess oxygen, thereby adding to the free Sn donor concentration. Additional contributions from oxygen vacancy donors are also possible.

With the use of doping and/or reduction, transport in the materials studied ranges from semiconducting behavior (undoped $In_2O_{3-\delta}$ and as-fired ITO) to transitional behavior (reduced $In_2O_{3-\delta}$) to metallic behavior (cosubstituted specimens). The reduced cosubstituted materials had carrier concentrations of $(3.2-7) \times 10^{20}$ cm^{-3} and mobilities of 13−14 $cm^2/V\cdot s$. Given that carrier concentration is roughly temperature independent in these materials, the linear temperature dependence of resistivity suggests that scattering increases and mobility decreases with increasing temperature, which is consistent with metallic behavior.

Acknowledgment. This work was supported by the MRSEC program of the National Science Foundation (DMR-0076097) at Northwestern University and made use of the Central Facilities of the same MRSEC program. George Palmer was supported by a National Defense Science and Engineering Graduate fellowship funded by the Office of Naval Research. Professor Jack Bass, Professor John Ketterson, and Dr. John Koenitzer provided helpful insights during discussion.

CM0100725